ELSEVIER

Available online at www.sciencedirect.com

SCIENCE DIRECT®

Electrochimica Acta 49 (2004) 1435–1444

ELECTROCHIMICA Acta

www.elsevier.com/locate/electacta

Photocatalytic reduction of Hg(II) on two commercial TiO_2 catalysts

Xiaoling Wang, S.O. Pehkonen, Ajay K. Ray*

Department of Chemical and Environmental Engineering, National University of Singapore, 10 Kent Ridge Crescent, Singapore 119260, Singapore

Received 20 June 2003; received in revised form 31 October 2003; accepted 31 October 2003

Abstract

The photocatalytic reduction of Hg(II) in air-equilibrated aqueous suspensions of TiO_2 under UV-illumination were studied. The amount of Hg(II) photo-reduced is affected by the pH of solution, the amount of the hole-scavengers, the concentration of chloride, mass of the catalyst, and incident light intensity. Hg(0) was detected during the photocatalytic reduction of Hg(II). The reduction rate of Hg(II) was controlled by the amount of Hg(II) adsorbed onto the TiO_2 powders. About 100 ppm Hg(II) is efficiently removed within 30 min from air-equilibrated solution at pH 4. The separation for Cr(VI)/Hg(II) mixtures can be achieved via UV/TiO_2 photocatalysis. Photocatalytic activities of two commercially available TiO_2 (Degussa P25 and Hombikat UV100) were also compared for different light intensities and catalyst loadings.

Keywords: Photocatalysis; Photocatalytic reduction; Mercury; TiO_2 catalyst

1. Introduction

For the past several decades, mercury (Hg), has received increasing attention as a serious pollutant due to its toxic and bio-accumulative properties [1]. In aquatic systems, mercury is often converted by bacteria to methylmercury (an organic form of mercury), which can be magnified through the aquatic food chain hundreds of thousands of times, posing a potential risk to humans and wildlife that consume fish [2]. The major sources of mercury pollution in the aquatic environment are industries, such as chloralkali, paint, electrical, rubber processing, oil refining, and fertilizer industry. In addition, coal combustion and waste incineration emit large quantities of mercury into the atmosphere.

Photocatalytic transformation or deposition of metals from aqueous solutions has been developed in environmental clean-up and remediation [3–5]. This photocatalytic method is based on the reactive properties of electron-holes pairs generated in the semiconductor particles upon illumination by light with energy greater than the semiconductor bandgap. For the deposition of a metal M, the energy of the semiconductor band electron must be more negative than the E^0 of the metallic couple (M^{n+}/M^0). Ag(I), Au(III), Cu(II), Pd(II), and Pt(IV) have been successfully converted to metallic form via semiconductor photocatalysis [6–10]. Photocatalytic reduction of Cr(VI) to Cr(III) utilizing a semiconductor has also been widely studied [11–15].

The objective of this study is to investigate the optimal parameters that affect the photocatalytic reduction of Hg(II) using TiO_2 powders. An interesting comparison study of photocatalytic activities of two commercial TiO_2 powders is also presented.

2. Materials and methods

Degussa P25 and Hombikat UV100 commercial titanium dioxide photocatalysts were employed in the experiments. Both catalysts were used without any pretreatment. The BET specific surface areas of Degussa P25 and Hombikat UV100 measured by nitrogen adsorption at −196 °C were found to be 43.8 and 249.0 m^2/g, respectively. Stock solutions of Cr(VI) and Hg(II) were prepared by dissolving analytical grade $K_2Cr_2O_7$ (Fluka) and $HgCl_2$ (Merck) in ultra-pure water, which has been passed through an 18 MΩ Milli-Q water purification system.

Batch adsorption experiments on TiO_2 were performed in the dark. The solution pH was adjusted by using dilute HNO_3 and NaOH. Photocatalytic experiments were carried out in a 200 ml cylindrical Teflon reactor at room temperature (295 ± 2 K). A 150 ml mixture inside the reactor was maintained in suspension by a magnetic stirrer. Irradiation was provided by a 450 W Xe arc lamp (Oriel Model 6266)

---

* Corresponding author. Tel.: +65-6874-8049; fax: +65-6779-1936.
E-mail address: cheakr@nus.edu.sg (A.K. Ray).

0013-4686/$ – see front matter © 2003 Elsevier Ltd. All rights reserved.
doi:10.1016/j.electacta.2003.10.030

with a UV-Vis band-pass filter (Oriel Model 59450) placed on the top of the reactor. The light emission is above the wavelength of 290 nm and the light intensity at the level of the reactor bottom is found to be ~2.2 mW cm^{-2} at 312 nm using a UVI*tec* RX-003 radiometer. This light was employed as incident light in most experiments. In the experiment of lower light intensity, a neutral density filter (Oriel Model 59680) was mounted on top of the band-pass filter. It can attenuate ~58% of the incident light intensity. In all the photocatalysis experiments described below, 5 mM of formic acid was added to the reactor unless stated otherwise. Formic acid is used to remove photo-generated holes in order to allow the reduction to proceed. Air-equilibrated suspensions were used in all experiments. The suspensions are initially maintained under agitation in the dark for 60 min to allow for an adsorption–desorption equilibrium to be established. During the irradiation, aliquots of the solution were withdrawn intermittently for analysis. All samples were filtered through a 0.45 μm Whatman Autovial filter before analysis.

Samples were analyzed for Cr(VI) using the 1,5-diphenylcarbazide method (Ueno et al., 1992) with a Shimadzu 1240 UV/VIS spectrophotometer. The detection limit of this method is 0.05 mg/l. Hg(II) concentrations were measured by ICP-OES (Inductively coupled plasma-optical emission spectroscopy, Perkin Elmer Optima 3000DV), because the samples for Hg(II) analysis were filtered and the results using ICP have no differences from those using the Dithizone method (Eaton et al., 1995). In order to prevent adsorption losses of mercury on the bottle walls, a gold preservative was added to every sample to yield 50 mg/l Au in the final volume. The detection limit for Hg by the ICP method is 1 μg/l.

Table 1
The percentage of Hg(II) adsorbed on the two TiO_2 catalysts

Catalyst[a]	pH		
	2.5	3	4
Degussa P25	1.8	4.5	12.3
Hombikat UV100	0.8	5.4	15.7

[a] $[TiO_2] = 2$ g/l.

In order to investigate the surface properties of two commercial TiO_2 powders, the ζ potential values of TiO_2 suspensions with different pH values were measured by a Brookhaven ZetaPlus zeta potential analyzer. X-ray photoelectron spectroscopy (XPS) was performed on the AXIS-His spectrometer (Kratos Analytical Ltd., UK) using a monochromatic Al Kα X-ray source (1486.6 eV photons) at a constant dwell time of 100 ms and a pass energy of 40 eV. C 1s signal (284.6 eV) was used as internal reference in all experiments. Prior to XPS measurements, the prepared samples were kept in the de-aerated desiccator to protect the samples from air.

3. Results and discussion

3.1. Adsorption of Hg(II) onto TiO_2

In order to investigate adsorption, a series of experiments in the dark at different pH values were carried out. It can

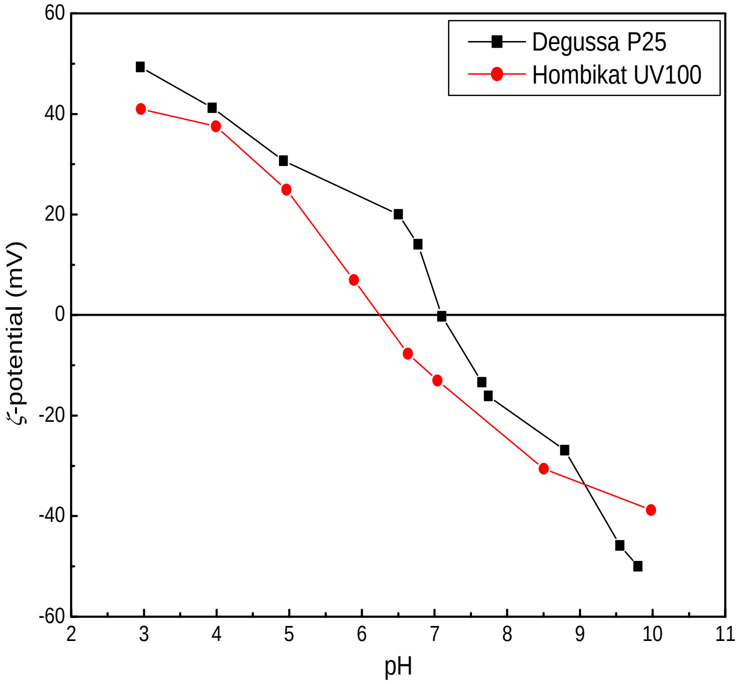

Fig. 1. ζ-Potential of the two TiO_2 suspensions as a function of pH at an ionic strength of 0.001 M $NaNO_3$.

be noticed that the adsorption of Hg(II) on the TiO_2 surface reached saturation within 1 h. Table 1 summarizes the results of adsorption experiments of 0.56 mM of Hg(II) using TiO_2 Degussa P25 and Hombikat UV100 as adsorbents. The amount of Hg(II) adsorbed by TiO_2 particles increased with increasing solution pH. The adsorption of the Hg(II) on TiO_2 depends to a great extent on the surface charge of TiO_2 particles. To investigate the surface properties of TiO_2 particles in water, the ζ-potential values of TiO_2 suspensions as a function of pH are presented in Fig. 1. The isoelectric point (pI), was ∼6.2 and 7.1 for Hombikat UV100 and Degussa P25, respectively. The pI of Degussa P25 is in agreement with the value of 7.0 obtained previously by Rodenas et al. [16]. But there is no reported pI value of Hombikat UV100 in the published literature. Therefore, TiO_2 particles are positively charged when pH is lower than 6.2 in the case of Hombikat UV100 and 7.1 in the case of Degussa P25. Moreover, the amount of positive charge decreases with increasing pH. This results in decreased electrostatic repulsion between the Hg^{2+} and the positively charged TiO_2 surface. Thus, the extent of adsorption of Hg(II) increased at higher pH values. It can also be noticed that the amount of adsorbed Hg(II) on Hombikat UV100 is larger than that on Degussa P25 except at the low pH 2.5. This is not only due to the higher surface area of Hombikat (249.0 m^2/g), but also the lower charge density on the surface of Hombikat compared with Degussa P25 at the same pH values (Fig. 1).

3.2. *Effect of pH on the photocatalytic reduction of Hg(II)*

A blank experiment of irradiating the solution containing Hg(II) at 0.56 mM without TiO_2 shows no decrease in Hg(II) concentration. The same result was obtained in another blank test on a reaction solution containing 20 mM of formic acid and 0.56 mM of Hg(II) without TiO_2 under UV irradiation. However, when TiO_2 particles were added into these two solutions, the white TiO_2 turned black with time, Hg(0) being produced as discussed below. Therefore, the photo-reduction of Hg(II) occurs only in the presence of the semiconductor powders. Fig. 2 depicts the results of Hg(II) photo-reduction as a function of irradiation time at different solution pH values in the presence of Degussa P25 TiO_2. Decreasing the pH decreased the amount of Hg(II) photo-reduced. It can be explained by the effect of solution pH on the potential of conduction band electrons and the surface properties of the TiO_2 semiconductor. The potential of the conduction band electron is pH dependent, and shifts to more cathodic potentials with increasing pH [17].

$$E_{CB} = -0.05 - 0.059\,\text{pH} \quad (\text{at } 25\,^{\circ}\text{C}) \tag{1}$$

The driving force for Hg(II) reduction by conduction band electrons thus increases as pH increases. On the other hand, it is considered that the mechanism of the photocatalytic reduction is based on the delivery and receipt of electrons between photo-excited TiO_2 and Hg ions adsorbed onto the TiO_2 surface [18]. The increasing amount of adsorbed Hg(II) on TiO_2 (Table 1) with an increase in solution pH makes additional Hg(II) ions available to react with photo-generated electrons on the TiO_2 surface. From Fig. 2, we can observe that by increasing the solution pH from 2.5 to 3, the rate of Hg(II) reduction increases significantly, yet the amount of Hg(II) adsorbed on the catalyst was only increased slightly (Table 1). It can be ascribed to the possible photo-oxidation of Hg(0), which inhibits the overall rate of Hg(II) reduction under strongly acidic condition by photo-generated holes. Serpone et al. [2] found Hg(II) reduction in the first 20 min of irradiation followed by the Hg(II) re-dissolution at pH 0 due to mercury(0) re-oxidation. The photo-oxidation of mercury(0) is thermodynamically favored at more acidic pH, because the potential of the valence band hole also shifts to more cathodic potentials with increasing solution pH.

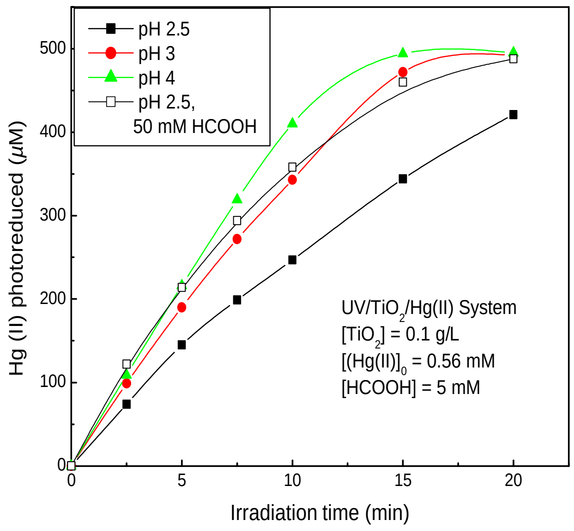

Fig. 2. The variation in the amount of Hg(II) photo-reduced with irradiation time at different pH using TiO_2 Degussa P25.

$$E_{VB} = 3.15 - 0.059\,\text{pH} \quad (\text{at } 25\,^{\circ}\text{C}) \tag{2}$$

Increasing the amount of formic acid in Hg(II) solution from 5 to 50 mM at pH of 2.5, as shown in Fig. 2, significantly increased the amount of Hg(II) reduced. However, the optimal value of the concentration of formic acid for Hg(II) reduction at pH 4 was found to be 5 mM (in Fig. 3), which indicates that the re-oxidation of Hg(0) occurs easily under strongly acidic conditions.

3.3. *Effect of HCOOH on the photocatalytic reduction of Hg(II)*

Preliminary experiments revealed a progressive increase in the amount of Hg(II) reduced at pH 4, thus all further experiments were carried out at this pH. It is well known that the overall quantum efficiency of photocatalysis is determined by the interfacial electron-transfer rate and the recombination lifetime of the photo-generated holes and electrons. To enhance the quantum efficiencies, the most

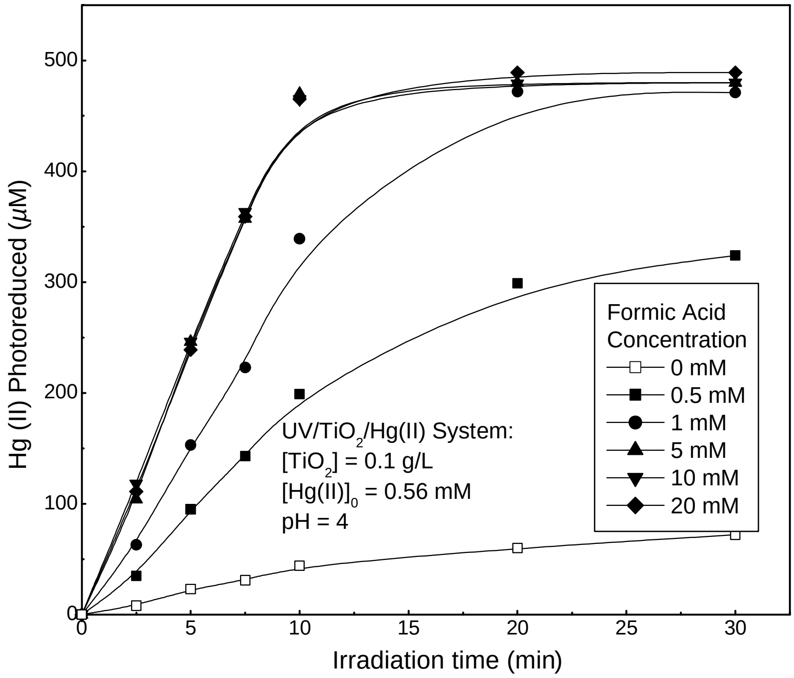

Fig. 3. The variation in the amount of Hg(II) photo-reduced with irradiation time as a function of formic acid concentration using TiO_2 Degussa P25.

common way is to increase the recombination lifetime of holes and electrons. Therefore, in the process of photocatalytic reduction of metal ions, filling the valence band holes by the electrons of the reductant may accelerate the photocatalytic efficiency. In the absence of organic species, the photo-generated holes would have to be consumed by water via a four-electron-pathway (Eq. (3)). However, this is a kinetically slow process [4].

$$2H_2O + 4h^+_{VB} \rightarrow O_2 + 4H^+ \qquad (3)$$

In order to complete the hole transfer efficiently, formic acid was selected as the hole scavenger in our experiments. There are three advantages for selecting formic acid: (a) Formic acid only absorbs light with wavelengths below 260 nm, as a consequence, there will be only photocatalytic (no direct photolysis) reactions involving formate under our experimental conditions; (b) formic acid is a small molecule, which is easily adsorbed onto TiO_2, so that direct oxidation by the hole may occur; and (c) the photoproducts of formic acid oxidation are CO_2 and H_2O,

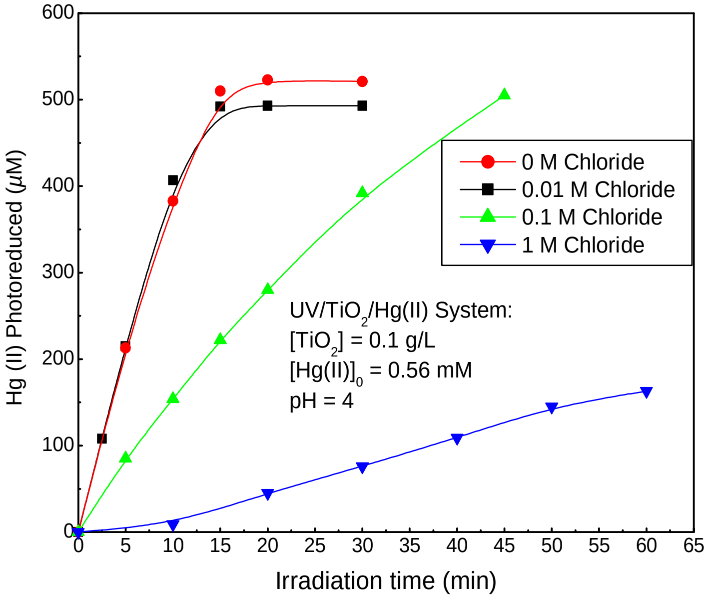

Fig. 4. The variation in the amount of Hg(II) photo-reduced with irradiation time as a function of chloride concentration using Degussa P25 TiO_2.

these products would not lead to troublesome environmental issues. One should also note that $OH^\bullet$ could react with formic acid and oxygen present in the solution to give superoxide, which further participates in the overall reaction process.

Fig. 3 illustrates the rather dramatic effect of formic acid on the photocatalytic reduction of Hg(II). The figure clearly shows that HCOOH can act as an efficient hole scavenger during the reaction. Carraway et al. [19] have provided experimental evidence for the direct oxidation of formate by the hole at the semiconductor surface. As shown in Fig. 3, formic acid accelerated the rate of Hg(II) reduction, even at concentrations as low as 0.5 mM. The rate increased significantly with the HCOOH concentration. However, when more than 5 mM of HCOOH is present in the solution, the reaction rate seemed to approach a limiting value. The identical profiles of Hg(II) reduced with irradiation time in the solution containing HCOOH at 5, 10, and 20 mM suggests that the efficiency of photocatalytic reduction of Hg(II) may be determined only by the rate of electron-transfer from TiO_2 surface to Hg(II) when HCOOH approaches a certain value, not by the recombination lifetime of electrons and holes.

It should be noted that all experiments were conducted in air-saturated samples. Inherent oxygen ($\approx 250 \times 10^{-6}$ M) in sample solutions is expected to successfully compete with Hg(II) for conduction band electron. This is expected since the rate constant for oxygen ($O_2 + e^-_{aq} \rightarrow O_2^{\bullet -}$, $k = 1.9 \times 10^{10}\,l\,mol^{-1}\,s^{-1}$ [20]) is slightly higher than Hg(II) reaction ($Hg(II) + e^-_{aq} \rightarrow Hg(I)$, $k = 7.1 \times 10^{9}\,l\,mol^{-1}\,s^{-1}$ [21]) with electron. Therefore, one can expect that in the absence of dissolved oxygen, by purging the solution with nitrogen, a higher removal rate of metal ions might be achieved. This was indeed found out to be true and was reported elsewhere [5].

3.4. Effect of chloride on the photocatalytic reduction of Hg(II)

Data for photocatalytic reduction of Hg(II) in the presence of varying chloride are shown in Fig. 4. A significant decrease in the photo-reduction rate of Hg(II) was observed as chloride concentration increased. This could be due to the mercury-chloride complexes which are present in water. If Hg^{2+} and Cl^- are present in water, they will combine to form the undissociated, but soluble species $HgCl_2$ (aq), where (aq) is used to designate that the species is in solution. Chloride can also combine with mercury in other proportions to form a variety of complexes, among which $HgCl^+$, $HgCl_3{}^-$, and $HgCl_4{}^{2-}$ are the predominant species. Equilibrium relationships for the various mercury-chloride species can be developed from the following reactions:

$$Hg^{2+} + Cl^- \rightleftharpoons HgCl^+ \quad K_1 = 5.6 \times 10^6 \tag{4}$$

$$HgCl^+ + Cl^- \rightleftharpoons HgCl_2 \quad K_2 = 3 \times 10^6 \tag{5}$$

$$HgCl_2 + Cl^- \rightleftharpoons HgCl_3{}^- \quad K_3 = 7.1 \tag{6}$$

$$HgCl_3{}^- + Cl^- \rightleftharpoons HgCl_4{}^{2-} \quad K_4 = 10 \tag{7}$$

where K_1, K_2, K_3, and K_4 are the stability constants [1]. Moreover, hydrolysis of these species can occur in the presence of OH^- [22].

$$Hg^{2+} + 2H_2O \rightleftharpoons Hg(OH)_2 + 2H^+ \quad K_5 = 10^{-6.09} \tag{8}$$

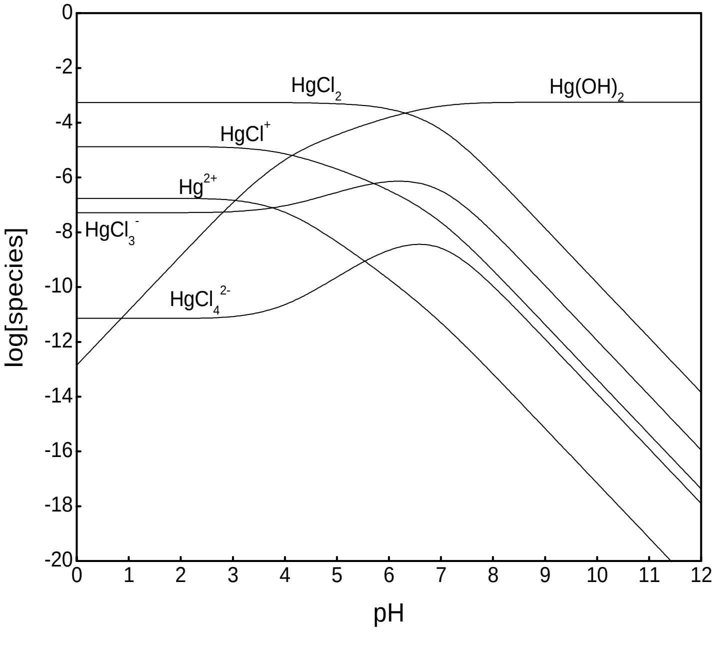

Fig. 5. Distribution of aqueous mercury species at 0.56 mM Hg(II) and 1.12 mM Cl^- as a function of pH.

Table 2
Hg(II) adsorbed on Degussa P25 TiO_2[a] in the presence of different concentrations of chloride at pH 4

NaCl in solution (M)	Hg(II) adsorbed (%)
0	10.7
0.01	5.2
0.1	2.0
1	1.3

[a] $[TiO_2] = 0.1$ g/l.

Based on the mass balance of reacting Hg(II) species using the appropriate stability constants, Fig. 5 illustrates the distribution of soluble mercury species in water as a function of pH when the total molar concentration of Hg(II) is 0.56 mM. At pH lower than 7, the predominant species in water is the neutral $HgCl_2$, not Hg^{2+}. As the chloride concentration increases, the amount of Hg^{2+} ion in the aqueous media would decrease, $HgCl_4{}^{2-}$ being the predominant species. However, the redox potential (versus NHE) of the Hg^{2+}/Hg couple is 0.85 V, which is higher than that of two mercuric chloride complexes ($E^0_{\mathrm{HgCl_4}^{2-}/\mathrm{Hg}} = 0.46\,\mathrm{V}$ and $E^0_{\mathrm{HgCl_2/Hg}} = 0.41\,\mathrm{V}$) [22], therefore, the photocatalytic reduction of Hg(II) is favored in the aqueous media containing a low concentration of chloride.

The effect of increasing chloride concentration on the rate of photocatalytic reduction of Hg(II) may also be due to the less active sites of TiO_2 catalyst available. Table 2 summarizes the adsorption of Hg(II) in the presence of chloride under the same experimental conditions in Fig. 4. The large amount of Cl^- in solution may result in the blocking of active surface sites on TiO_2, since the positively charged TiO_2 surface at pH 4 contributes to Cl^- adsorption.

3.5. Separation of Cr(VI)/Hg(II) mixtures

The addition of Cr(VI) to TiO_2 suspension dramatically inhibited the initial Hg(II) reduction rate as shown in Fig. 6. The redox potential (versus NHE) of $Cr_2O_7{}^{2-}/Cr^{3+}$ is 0.82 V at pH 4; it can compete more favorably with $HgCl_2$ for electrons. The inhibitory effect of Cr(VI) on Hg(II) reduction by the UV/TiO_2 process may also be attributed to catalyst deactivation, consider that although Cr(VI) has been converted to Cr(III) after 60 min of irradiation (in Fig. 5), the rate of Hg(II) reduction was still slow at this stage. To verify this hypothesis, we have filtered the suspension after 60 min of irradiation in order to remove the used catalyst and to replace it with fresh TiO_2 at 2 g/l of the remaining solution. As shown in Fig. 5, after 10 additional minutes of irradiation, the reduction of Hg(II) is almost complete. It can be concluded that Cr(III) species depositing on the TiO_2 surface after Cr(VI) photo-reduction results in the loss of TiO_2 photocatalytic activity.

The effect of Cr(VI) on Hg(II) reduction suggests that photocatalysis is a useful technique for the separation of Hg(II)/Cr(VI) mixtures, which exist in the dental office waste stream. Since soluble chlorides can act as legends to form complexes with mercury, which have lower reduction potentials than Hg^{2+}, the proper addition of chlorides to a Hg(II)/Cr(VI) mixture can retard the photocatalytic reduction of Hg(II) and achieve a good final mercury recovery with insignificant traces of other toxic metals, such as Cr(VI).

3.6. Comparison of photocatalytic activities of TiO_2 degussa P25 and hombikat UV100

TiO_2 Degussa P25 and Hombikat UV100 were tested for the photocatalytic reduction of Hg(II) at pH 4. Fig. 7

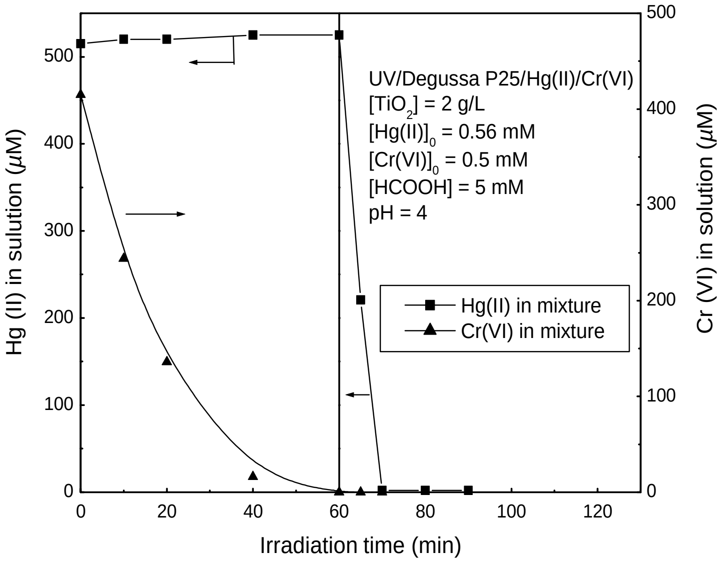

Fig. 6. The effect of Cr(VI) on the photocatalytic reduction of Hg(II).

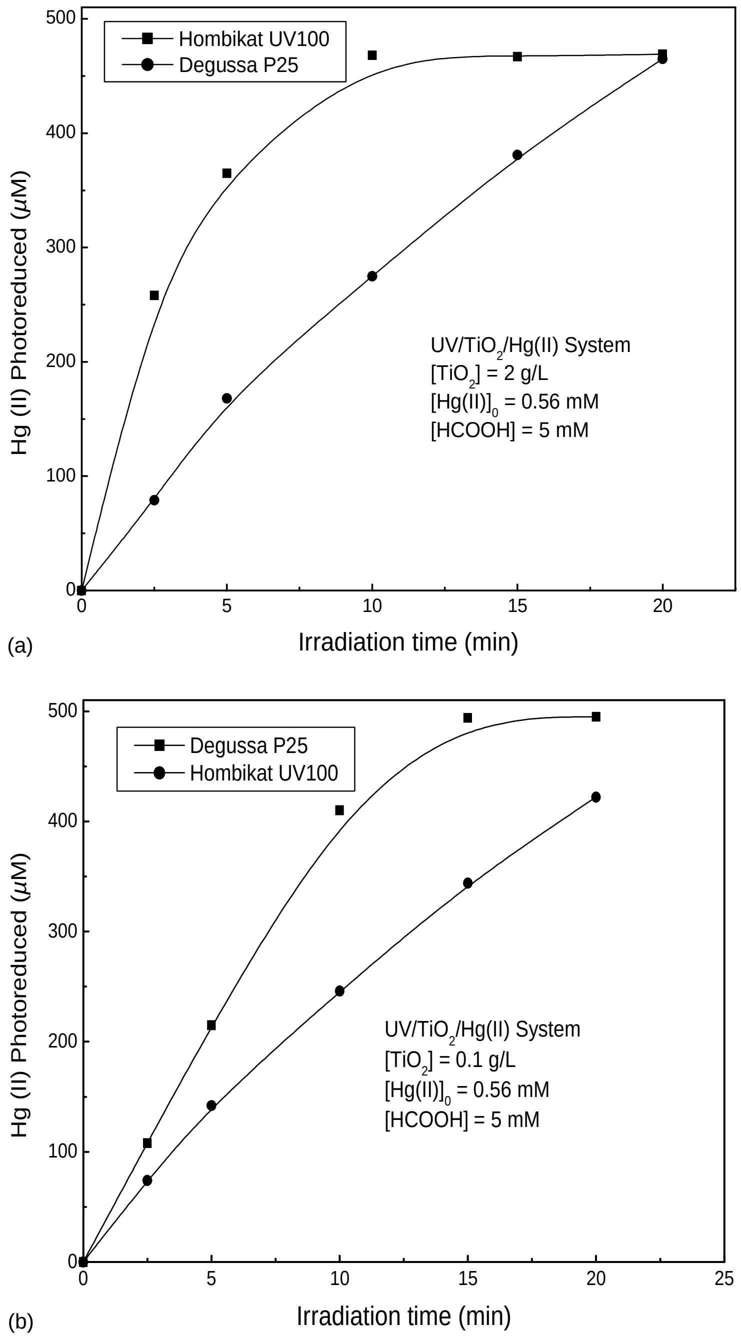

Fig. 7. The comparison in the amount of Hg(II) photo-reduced with irradiation time for two different commercial TiO_2 powders.

shows the photo-reduction of Hg(II) for two different brand of catalyst with illumination time at same experimental conditions except amount of catalyst. When 2 g/l catalyst is used (Fig. 7a), the photo-reduction of Hg(II) proceeded to completion within 10 min when Hombikat UV100 TiO_2 is used, while only a half of the amount of Hg(II) has been reduced using Degussa P25 during the same time. However, photo-reduction was almost complete in 20 min. This may be due to the higher surface area of Hombikat UV100, thus more active sites taking part in the reduction process. Similar experimental results were reported by Khalil et al. [23]. However, when the TiO_2 dose was reduced (Fig. 7a) from 2 to 0.1 g/l (Fig. 7b), the photocatalytic activity of Degussa P25 was higher than that of Hombikat UV100. It indicates that the two commercial TiO_2 powders may have a different sensitivity to the incident light intensity, since the dose of the catalyst would influence the light absorbance. Degussa P25 is composed of loose aggregates of TiO_2, whereas Hombikat UV100 particles are highly agglomerated TiO_2 [14]. Therefore, the Degussa P25 TiO_2 suspension is more opaque than Hombikat UV100 when the catalyst loading is 2 g/l. This results

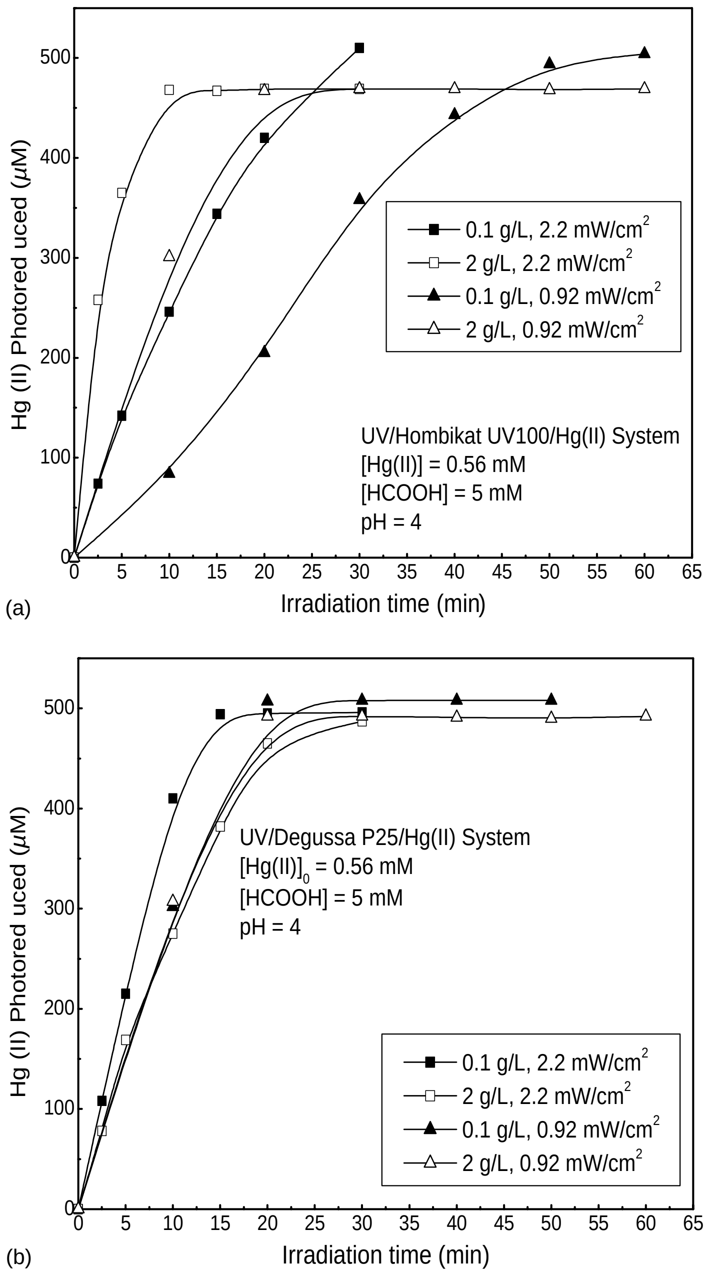

Fig. 8. The effect of incident light intensity and TiO_2 dosage on photocatalytic reduction of Hg(II) using: (a) Hombikat UV100; (b) Degussa P25.

in lower light penetration through the Degussa P25 TiO_2 suspension.

To compare the effect of incident light intensity on two commercial TiO_2 catalysts, the experiments of Hg(II) reduction in two UV/TiO_2 systems were carried out under the same conditions. Fig. 8a shows the conversion of Hg(II) using Hombikat UV100. The results indicate that, at a certain dose of Hombikat UV100, the rate of Hg(II) reduction increased with increasing light intensity. On the other hand, the rate also increased with the dose of Hombikat UV100. These results are similar to those of Khalil et al. [23]. They found that the optimum dose of Hombikat UV100 was 2 g/l. However, we did not observe a significant improvement of Hg(II) reduction using Degussa P25 when the light intensity was increased. By raising the incident light intensity from 0.92 to 2.2 mW/cm^2, the rate of Hg(II) reduction increased only slightly, whether the dose of Degussa P25 was as high as 2 g/l or as low as 0.1 g/l (Fig. 8b). It seems Degussa P25 has already reached its limiting capacity for light absorbance, while Hombikat UV100 has not reached it yet. Moreover, unlike Hombikat UV100, the reduction rate of Hg(II) in a 2 g/l Degussa P25 suspension was smaller than in a 0.1 g/l suspension. It is suggested that the optimum dose of Degussa P25 has shifted to a lower value, not the reported 2 g/l. This probably occurs due to the light shadowing (shielding) effect of a large amount of dark Hg(0) deposited

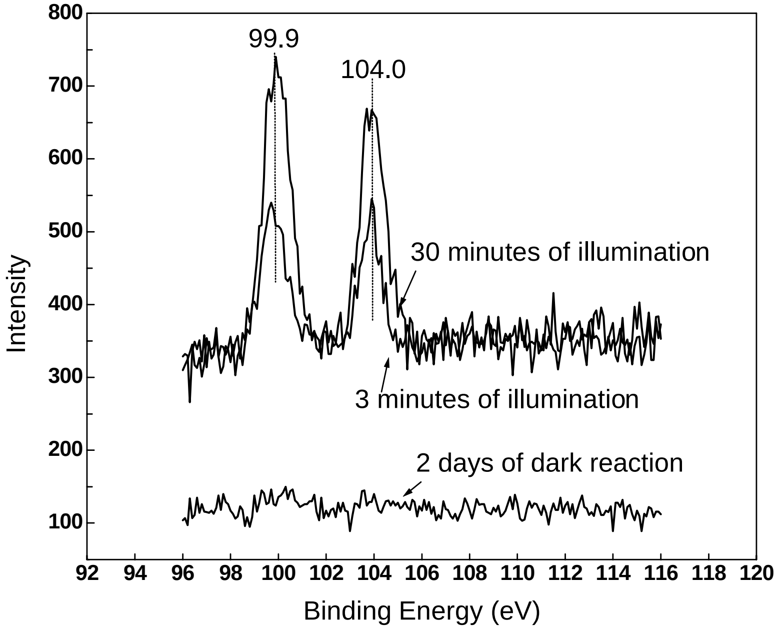

Fig. 9. Hg(4*f*) XPS spectra of the surface TiO_2 Degussa P25.

on the TiO_2 surface. The above results clearly show that the photocatalytic activity depends in addition to the selection of brand of catalyst, also on catalyst loading and light intensity. Degussa P25 is photo-catalytically more active than Hombikat UV100 at the low catalyst loading and at low light intensity.

3.7. XPS study

Photo-reduction of metal ions on semiconductor surfaces has been studied extensively using many advanced techniques. Based on the EPR (electron paramagnetic resonance) study, Rajh et al. [24] proposed the current doubling mechanism for lead reduction on surface-modified TiO_2 nano-particles. XAFS was also used by Chen et al. [25] to investigate the photo-reduction of heavy metal ions, Cu^{2+}, Hg^{2+} on TiO_2 nano-particle surfaces. In this study, XPS is used to identify the oxidation state of mercury in our experiments. Since XPS is sensitive to the oxidation state as well as the local environment of the metal, it provides a positive identification of the metal speciation.

The used TiO_2 after adsorption or photocatalytic reduction of Hg(II) at pH 4 were analyzed by XPS. Fig. 9 shows that Hg(4*f*) was not detected on the TiO_2 surface after 2 days of adsorption. This may be ascribed to the small amount of Hg(II) adsorbed on the TiO_2 surface at pH of 4. However, two sharp peaks of Hg(4*f*) appeared after 3 min of UV-illumination. The $4f_{7/2}$ and $4f_{5/2}$ binding energies were measured to be 99.9 and 104.0 eV, respectively. Comparing with the data from the literature [26,27], Hg(4*f*) signals in Fig. 9 could be assigned to Hg(0) species, while no indication of the presence of Hg(I) was observed. The intensity of signals increased with illumination time as shown in Fig. 9. This is strong evidence that under UV-illumination, the amount of Hg(II) reduced on the TiO_2 is increasing.

4. Conclusions

Hg(II), a toxic species in aquatic systems, can be photo-reduced via the UV/TiO_2 process. The process is an efficient route for the removal or the recovery of mercury, since increasing the pH and the amount of catalyst used can increase the rate of the reduction process. The addition of an organic hole scavenger also increases the photo-reduction rate. Mercury can be selectively and totally reduced and extracted from a Cr(VI)/Hg(II) mixture in the presence of chloride. Degussa P25 is found to be photo-catalytically more active than Hombikat UV100 at the low catalyst loadings and at low light intensities. In this study, optimal parameter values of pH of solution, mass of the catalyst, incident light intensity, amount of the hole-scavengers, and the concentration of chloride on the rate of photocatalytic reduction process of Hg(II) are determined.

References

[1] C.N. Sawyer, P.L. McCarty, G.F. Parkin, Chemistry for Environmental Engineering, McGraw-Hill, New York, 1994, p. 10
[2] N. Serpone, Y.K. Ah-You, T.P. Tran, R. Harris, E. Pelizzetti, H. Hidaka, Sol. Energy 39 (1987) 491.
[3] J.M. Herrmann, Catal. Today 53 (1999) 115.
[4] M.I. Litter, Appl. Catal. B 23 (1999) 89.
[5] D.W. Chen, A.K. Ray, Chem. Eng. Sci. 56 (4) (2001) 1561.
[6] M.D. Ward, A.J. Bard, J. Phys. Chem. 86 (1982) 3599.

[7] J.M. Herrmann, J. Disdier, P. Pichat, J. Catal. 113 (1988) 72.

[8] M. Bideau, B. Claudel, L. Faure, M. Rachimoellah, Chem. Eng. Commun. 93 (1990) 167.

[9] A. Caballero, A.R. Gonzalez-Elipe, A. Fernandez, J.-M. Gerrmann, H. Dexpert, F. Villain, J. Photochem. Photobiol. A: Chem. 78 (1994) 169.

[10] M.R. Prairie, L.R. Evans, B.M. Stange, S.L. Martinez, Environ. Sci. Technol. 27 (1993) 1776.

[11] J. Doménech, J. Munoz, Electrochim. Acta 32 (1987) 1383.

[12] W. Lin, W. Chang, K. Rajeshwar, J.Electrochem. Soc. 140 (1993) 2477.

[13] L.B. Khalil, W.E. Mourad, M.W. Rophael, Appl. Catal. B: Environ. 17 (1998) 267.

[14] G. Colón, M.C. Hidalgo, J.A. Navío, J. Photochem. Photobiol. A: Chem. 138 (2001) 79.

[15] X. Wang, S.O. Pehkonen, A.K. Ray, Complete Removal of Aqueous Cr(VI) by Combination of Photocatalytic Reduction and Co-precipitation, Industrial and Engineering Chemistry Research, in press, 2003.

[16] L.A.G. Rodenas, A.D. Weisz, G.E. Magaz, M.A. Blesa, J. Colloid Interface Sci. 230 (2000) 181.

[17] Y. Xu, M.A.A. Schoonen, Am. Mineral. 85 (2000) 543.

[18] S. Sanuki, K. Shako, S. Nagaoka, H. Majima, Mater. Trans. JIM 41 (2000) 799.

[19] E.R. Carraway, A.J. Hoffmann, M.R. Hoffmann, Environ. Sci. Technol. 28 (1994) 786.

[20] G.V. Buxton, C.L. Greenstock, W.P. Helman, A.B. Ross, J. Phys. Chem. Ref. Data 17 (1998) 513.

[21] E. Liu, I.E. Makarov, A.K. Pikaev, High Energy Chem. 17 (1983) 41.

[22] A.J. Bard (Ed.), Encyclopedia of Electrochemistry of the Elements, vol. 9, Marcel Dekker,New York, 1982, p. 2.

[23] L.B. Khalil, M.W. Rophael, W.E. Mourad, Appl. Catal. B: Environ. 36 (2002) 125.

[24] T. Rajh, A.E. Ostafin, O.I. Micic, D.M. Tiede, M.C. Thurnauer, J. Phys. Chem. 100 (1996) 4538.

[25] L. Chen, T. Rajh, Z. Wang, M.C. Thurnauer, J. Phys. Chem. B 101 (1997) 10688.

[26] J.F. Moulder, W.F. Stickle, P.E. Sobol, K.D. Bomben, Handbook of X-ray Photoelectron Spectroscopy: A Reference Book of Standard Spectra for Identification and Interpretation of XPS Data, in: J. Chastain (Ed.), Eden Prairie, Minnesota, Perkin-Elmer Corporation, Physical Electronics Division, 1992.

[27] B.V. Crist, Handbook of Monochromatic XPS Spectra, Wiley, New York, 2000.